

## HYDROCARBON SEEPAGE AND CARBONATE MOUND FORMATION: A BASIN MODELLING STUDY FROM THE PORCUPINE BASIN (OFFSHORE IRELAND)

J. Naeth<sup>1,2\*</sup>, R. di Primio<sup>2,5</sup>, B. Horsfield<sup>2</sup>, R.G. Schaefer<sup>1</sup>,  
P.M. Shannon<sup>3</sup>, W.R. Bailey<sup>3</sup> and J.P. Henriët<sup>4</sup>

*This study assesses whether the growth of deep water carbonate mounds on the continental slope of the north Atlantic may be associated with active hydrocarbon leakage. The carbonate mounds studied occur in two distinct areas of the Porcupine Basin, 200 km offshore Ireland, known as the Hovland-Magellan and the Belgica areas.*

*To evaluate the possible link between hydrocarbon leakage and mound growth, we used two dimensional cross-section and map-based basin modelling. Geological information was derived from interpretation of five seismic lines across the province as well as the Connemara oilfield. Calibration data was available from the northern part of the study area and included vitrinite reflectance, temperature and apatite fission track data.*

*Modelling results indicate that the main Jurassic source rocks are mature to overmature for hydrocarbon generation throughout the basin. Hydrocarbon generation and migration started in the Late Cretaceous. Based on our stratigraphic and lithologic model definitions, hydrocarbon migration is modelled to be mainly vertical, with only Aptian and Tertiary deltaic strata directing hydrocarbon flow laterally out of the basin. Gas chimneys observed in the Connemara field were reproduced using flow modelling and are related to leakage at the apices of rotated Jurassic fault blocks. The model predicts significant focussing of gas migration towards the Belgica mounds, where Cretaceous and Tertiary carrier layers pinch out. In the Hovland-Magellan area, no obvious focus of hydrocarbon flow was modelled from the 2D section, but drainage area analysis of Tertiary maps indicates a link between mound position and shallow Tertiary closures which may focus hydrocarbon flow towards the mounds.*

### INTRODUCTION

Carbonate mounds of varying size and shape are found in a variety of locations on the seabed. Reefs are normally associated with warm tropical waters

(Bathurst, 1975); however, modern platform carbonates can accumulate in seawater which is generally colder than 20°C (James, 1997). The use of submersibles and underwater cameras has led to the discovery of a series of cold water carbonate build-ups in areas such as the Cobb Seamount, NE Pacific (Farrow and Durant, 1985), the SE Brazilian continental slope (Viana *et al.*, 1994), the West Florida Slope (Neumann *et al.*, 1977), the Bahama Bank slopes (Mullins *et al.*, 1981), the Blank Plateau (Stetson *et al.*, 1963), the Rockall Bank (Wilson, 1979), the Porcupine Bank (Scoffin and Bowes, 1988), the Faroe Islands (Frederiksen *et al.*, 1992), offshore mid-Norway (Mortensen *et al.*, 1995), and the Norwegian fjords (Stromgren, 1974).

Seepage along faults and fractures or by means of diffusion is known to release gaseous and liquid hydrocarbons into seawater. Slightly below the

<sup>1</sup> Forschungszentrum Jülich GmbH, ICG-4 D-52425 Jülich, Germany.

<sup>2</sup> GeoForschungsZentrum Potsdam, Telegrafenberg, D-14473 Potsdam, Germany.

<sup>3</sup> University College Dublin, Department of Geology, Dublin 4, Ireland.

<sup>4</sup> Renard Centre of Marine Geology, University of Gent, B9000 Gent, Belgium.

<sup>5</sup> author for correspondence, dipri@gfz-potsdam.de

\* Present Address: Fugro Robertson Limited, Tyn-y-coed Site, Llanrhos, Llandudno, North Wales, LL30 1SA. jochen.naeth@fugro-robertson.com

sediment/seawater interface,  $\text{CO}_2$  is formed by the microbial anaerobic oxidation of both indigenous sedimentary organic matter and migrating hydrocarbons (predominantly methane) in the bacterial sulphate reduction zone (Suess and Whiticar, 1989). Specifically, chemo-synthetic bacteria use sulphate as an electron acceptor to oxidise the reduced carbon species (Hovland, 1990). This bacterial flora is the basis of a complex local food-web involving micro-organisms, filter-feeders and scavengers (Grassle, 1985). One result of this process is the precipitation of authigenic carbonates as crusts or concretions at the sediment/water interface (Ritger *et al.*, 1987). Such hydrocarbon-derived, vent-related carbonate hardgrounds or build-ups are typical by-products of microbial chemosynthesis and have been termed “chemoherms” (Roberts and Aharon, 1994). This stable substrate can be used by corals to settle and grow (e.g. *Lophelia* sp: Wilson, 1979) and may act as the foundation for a carbonate mound.

In this study, we investigate the Porcupine Basin, offshore Ireland, where numerous carbonate mounds up to 3 km long and with a maximum height of about 600 m have been recognized (de Mol *et al.*, 2002; Henriët *et al.*, 2001; Henriët *et al.*, 2003; Huvenne *et al.*, 2002; Huvenne *et al.*, 2003) (Fig.1). Of special interest are the “Hovland-Magellan” mound province on the northern slope of the Porcupine Basin, and the “Belgica” mound province on the eastern slope. Numerous buried and surface mounds were discovered by seismic methods during the Hovland-Magellan survey and during a survey with the R/V Belgica in 1997 (Henriët *et al.*, 1998).

The object of this study was to investigate whether these cold-water carbonate mounds form a “coupled” system with fluid flow processes in underlying strata, as originally proposed by Hovland (1990). Its purpose was to determine the timing and extent of hydrocarbon generation, to assess the composition of the hydrocarbons generated, and to investigate whether hydrocarbon migration is focussed towards the carbonate mounds. Numerical models were used to simulate hydrocarbon formation and migration.

## METHODS: NUMERICAL SIMULATION

Numerical basin modelling is based on the description and calculation of relevant geological processes occurring during the evolution of sedimentary basins (Poelchau *et al.*, 1997). In this study, the simulation programme *PetroMod*<sup>®</sup> (version 7.1, Integrated Exploration Systems GmbH, Germany) was used. The programme uses a forward modelling approach to calculate the geological and thermal evolution of a system in time and space. The simulation predicts the occurrence and composition of petroleum, and

reconstructs the main chemical and physical processes involved in the deposition of a potential source rock, the hydrocarbon generation history, migration processes and accumulation in possible traps. This workflow allows a quantitative evaluation of the geological and thermal evolution of the study area. The Easy%Ro kinetic description of vitrinite maturation (Sweeney and Burnham, 1990) was used to calculate vitrinite reflectance in the basin models.

## MODEL DEFINITION

### Conceptual Model

Five 2D cross-sections, based on seismic data, were modelled in this study. The locations of the lines modelled are shown in Fig.1. Seismic lines *RE25*, *RE94* and *RE88* were used to develop a regional understanding of basin evolution, whereas refined interpretations of lines *RE94*, *PORC97-12* and *CS2* were used for detailed migration modelling.

Profiles *RE25*, *RE94*, *RE88*, *PORC97-12* and *CS2* were vertically subdivided into layers, each of which represent discrete stratigraphic units. Fourteen horizons were interpreted: 1. seabed; 2. Pliocene; 3. mid- Miocene; 4. lower-Miocene; 5. base Miocene; 6. base Oligocene; 7. base Tertiary; 8. base chalk; 9. base Albion; 10. base Aptian; 11. Tertiary sills; 12. the Volcanic Centre; 13. base Cretaceous; and 14. base mid-Jurassic. Stratigraphic units below the mid-Jurassic could not be traced because of poor seismic resolution; the thicknesses of these units vary through the basin but were tied to wells in the *Connemara* vicinity and are assumed to be constant throughout the basin.

The tectono-stratigraphic evolution of the basin includes three phases of uplift together with erosional events in the Late Jurassic/Early Cretaceous and Tertiary (Shannon and Jacob, 1998; Shannon and Naylor, 1998). Erosion in the Late Jurassic/Early Cretaceous removed approximately 600 m of sediment; at the end of the Eocene, approximately 250 m were eroded; and at the end of the Oligocene, approximately 200 m of sediment were removed. These erosional episodes are only documented for the northern part of the basin where well control exists, and represent average values. In our models, we assumed that erosion was at a maximum at the basin margins and decreased to zero towards the basin centre (linear interpolation). At the end of the Cretaceous, a period of non-sedimentation occurred. Five million years after deposition of the Cretaceous chalk, Paleocene uplift occurred with prograding deltas and an increasing terrestrial influence.

Lithological definitions were based on well data (Shannon and Naylor, 1998) and extrapolated to the seismic cross-sections.

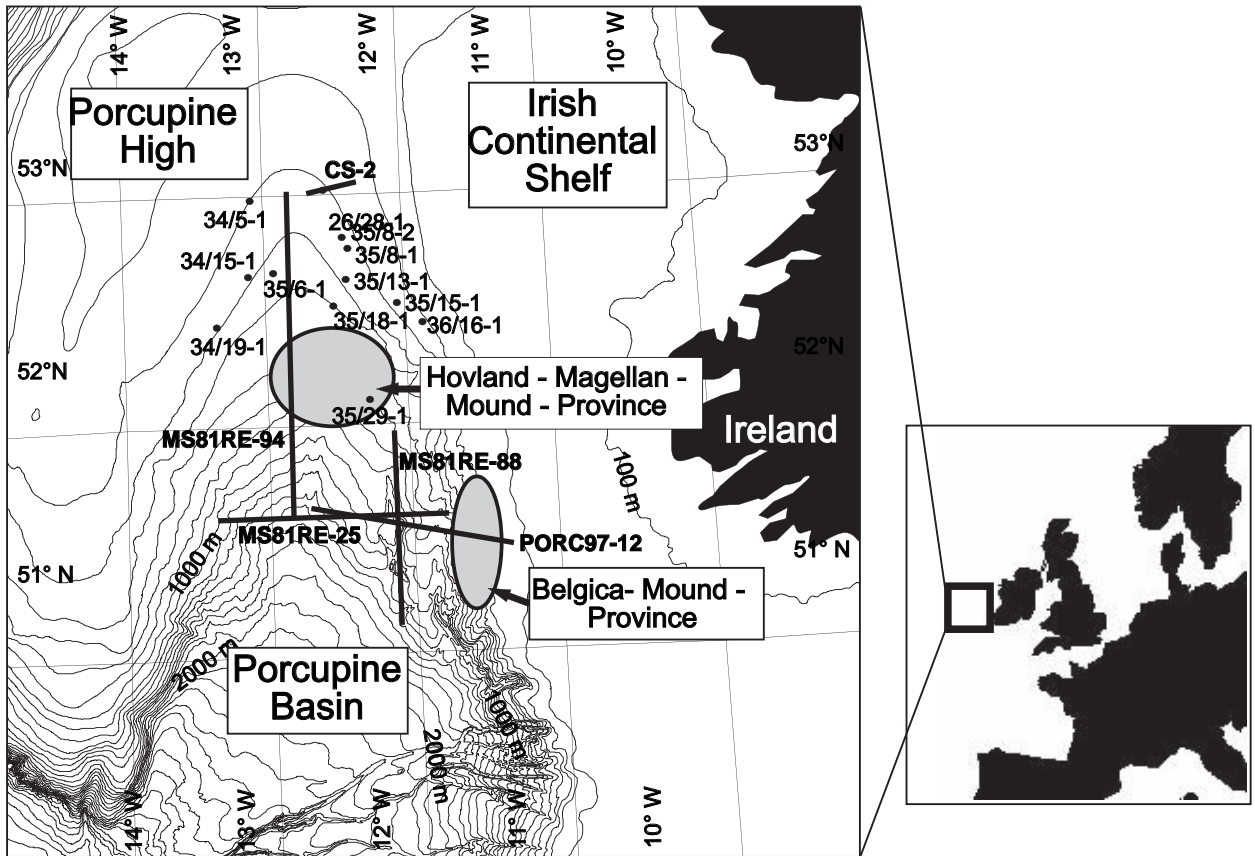


**Fig. 1.** Map of the Porcupine Basin showing the location of mound provinces (grey ovals), wells and seismic lines; water depths in 100 m contours.

Absolute ages were needed for each event. Only a few absolute age determinations have been performed on sediments in the Porcupine Basin (Tate and Dobson, 1988). Therefore, ages were defined according to the chronostratigraphic classification of the respective sequences. The ages were defined based on the timescale of Gradstein and Ogg (1996) combined with absolute age determinations from Tate and Dobson (1988).

The basic conceptual model is presented in Table 1. The age, lithology, environment, sea-level and tectonic history are given for each horizon beginning with the Jurassic sequences.

Modelling the generation and migration of hydrocarbons requires a definition of source rock occurrence and potential in the study area. Potential source rock intervals range from the Carboniferous to the Tertiary (Butterworth *et al.*, 1999; Croker and Shannon, 1987; Croker and Shannon, 1995; Moore and Shannon, 1995). Four discoveries have been made in the *Connemara* oilfield and several other exploration wells have reported oil and gas shows. A marine Upper Jurassic sequence is reported to be the best oil-prone source rock (Croker and Shannon, 1987), with maximum TOC values around 3–4 wt %. Middle Jurassic shales also have locally good oil and gas potential with TOC values up to 1.8 wt %

(Shannon and Naylor, 1998) and contain, together with Ryazanian to Aptian marine shales, an amorphous oil-prone kerogen type. They are, however, only of minor volumetric importance. Aptian – Albian shales with TOC values of up to 2.7 wt % have fair oil-generating potential. The Lower Tertiary coaly, lignitic and shaly deltaic sequences contain abundant terrestrial organic matter (TOC values of up to 50.5 wt %) and are considered predominantly gas-prone.

A reconstruction of the Middle to Late Jurassic palaeo environment has indicated that non-marine conditions prevailed in the northern part of the Porcupine Basin from at least Bathonian until well into Kimmeridgian time, whereas the southern part was fully marine (Butterworth *et al.*, 1999). Fluvial and coastal plain channel sandstones in the northern part of the basin are interbedded with lacustrine shales and deltaic sandstone; this entire facies assemblage (Butterworth *et al.*, 1999) reflects the periodic development of shallow lakes with the preservation of sand-prone lacustrine deltas and periodic algal blooms. These lacustrine shales are very good oil-prone source rocks with TOC values from 1.5 – 4 wt % and Hydrogen Indices (HI) > 500 mgHC/g TOC, and are similar to equivalents in the Jeanne d'Arc Basin, offshore Newfoundland (Butterworth *et al.*, 1999).

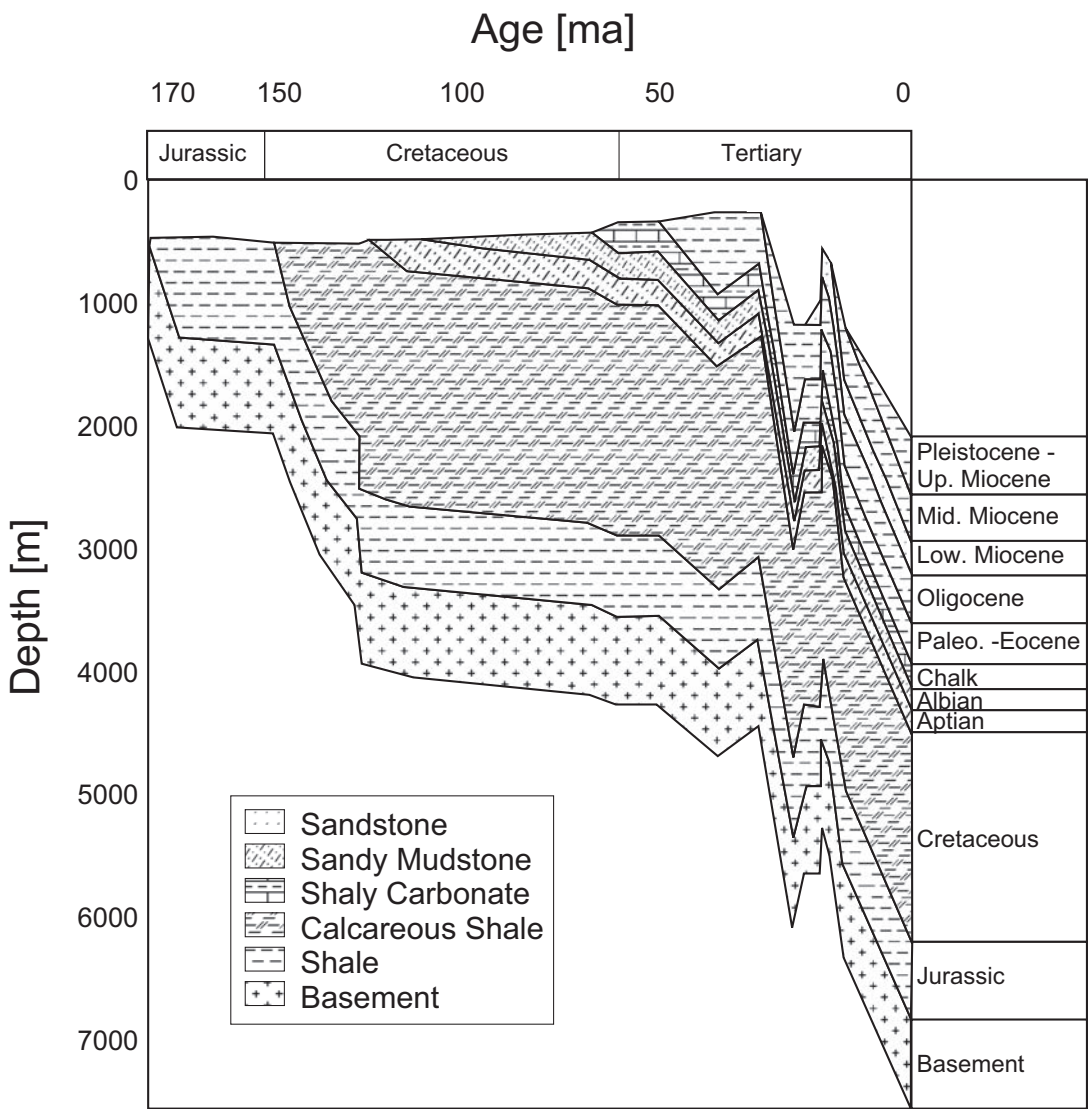


**Fig.2. Simplified burial history of line RE94 at its intersection with line RE25 showing Late Jurassic / Early Cretaceous fault-controlled subsidence, basin filling, Early Tertiary uplift and ongoing subsidence.**

For the conceptual model, the Upper Jurassic strata were defined as the main source rock with TOC values of 4 wt % and an HI of 550 mgHC/g TOC. In addition, source rock properties were assigned to the Lower Jurassic with TOC values of 1.7 wt % and an HI of 550 mgHC/g TOC.

A correct reconstruction of the geometric evolution of the model is required for the simulation of petroleum migration, as changes in carrier topography through time will significantly alter drainage patterns. In a basin model, the surface topography at any timestep represents the upper boundary condition with respect to the timestep's geometry. Therefore, palaeo water depth maps were determined for each time step modelled. As shown in the conceptual model, palaeo water depth values were available for the northern margin of the basin. In combination with the present-day geometry of individual layers and palaeo depositional information, the palaeo geometry was calculated by scaling the present-day depth of each

mapped top to the known palaeo water depth of these layers at well positions.

The first simulation of the burial history of the study area was performed using the input data described above. Fig.2 shows the burial history of line RE94 at the intersection with line RE25 (see Fig.1). Following Late Jurassic and Early Cretaceous fault-controlled subsidence, the basin was progressively filled with sediment until the present day. The only interruption to the subsidence occurred during the Paleocene, when thermal uplift took place due to the Iceland Plume (MacLennan *et al.*, 2001) and ridge push effects (Clift *et al.*, 1998). This overall burial history is similar for the three regional lines studied.

**Calibration**

For further evaluation of the petroleum systems in the Porcupine Basin, the thermal history of the study



| Horizon name      | Age (Ma) | Lithology | Environment                      | Source Rock | Sea-level                | Palaeo-water Depth (m) | Tectonic events                                 |
|-------------------|----------|-----------|----------------------------------|-------------|--------------------------|------------------------|---|
|                   | from     | to        |                                  |             |                          |                        |   |
|                   |          |           |                                  |             |                          |                        |   |
|                   |          |           |                                  |             |                          |                        |   |
| Pliocene (C10)    | 5.3      | 0.0       | mudstone                         |             |                          | 0->500                 |   |
| Miocene sills     | 20.3     |           | basalt                           |             |                          |                        |   |
|                   |          |           |                                  |             |                          |                        |   |
| Mid Miocene (C20) | 14.8     | 5.3       | mudstone                         |             |                          | 0->500                 |   |
|                   |          |           | mudstone - occasional sandstones |             |                          | 0->500                 | Alpine deformation pulse and ridge push effects |
| Base Miocene      | 23.8     | 14.8      |                                  |             |                          |                        |   |
| Erosion           | 26.0     | 23.8      |                                  |             | 200 m                    |                        |   |
| Oligocene (C30)   | 33.7     | 26.0      | mudstone                         |             | relative sea-level fall  | 0-200                  |   |
| Erosion           | 43.0     | 33.7      |                                  |             | 250 m                    |                        |   |
|                   |          |           |                                  |             |                          |                        |   |
| Eocene            | 54.8     | 43.0      | mudstone                         |             |                          | 0-60                   |   |
|                   |          |           |                                  |             |                          |                        |   |
| Paleocene/Eocene  | 56.0     | 54.8      | coaly-sandy-shaly                |             |                          | 0-61                   |   |
| Hiatus            | 60.9     | 56.0      |                                  | X           |                          |                        | Iceland plume related uplift                    |
|                   |          |           |                                  |             |                          |                        |   |
| Chalk             | 71.3     | 60.9      | marl                             |             |                          | <60-200                |   |
|                   |          |           |                                  |             | eustatic sea-level fall  |                        |   |
| Base Albian Sands | 112.0    | 71.3      | sandstone                        |             |                          | 0-200                  |   |
|                   |          |           |                                  |             |                          |                        |   |
| Base Aptian       | 121.0    | 112.0     | mudstone                         |             |                          | 0-500                  |   |
| Volcanic ridge    | 142.0    | 135.0     | basalt                           |             |                          |                        |   |
|                   |          |           |                                  |             |                          |                        |   |
| Base Cretaceous   | 140.0    | 121.0     | mudstone                         |             |                          | 0-500                  |   |
| Erosion           | 150.0    | 140.0     |                                  |             | fault related subsidence |                        | rifting during Mid-Cretaceous                   |
|                   |          |           |                                  |             | 600 m                    |                        |   |
| Upper Jurassic    | 180.0    | 150.0     | mudstone                         | X           | fault related subsidence | 0->200                 | rifting during Late Jurassic                    |
| Lower Jurassic    | 205.0    | 180.0     | mudstone                         |             |                          | >200                   |   |

Table 1. Conceptual model of the geological history and stratigraphic input parameters for the Porcupine Basin.



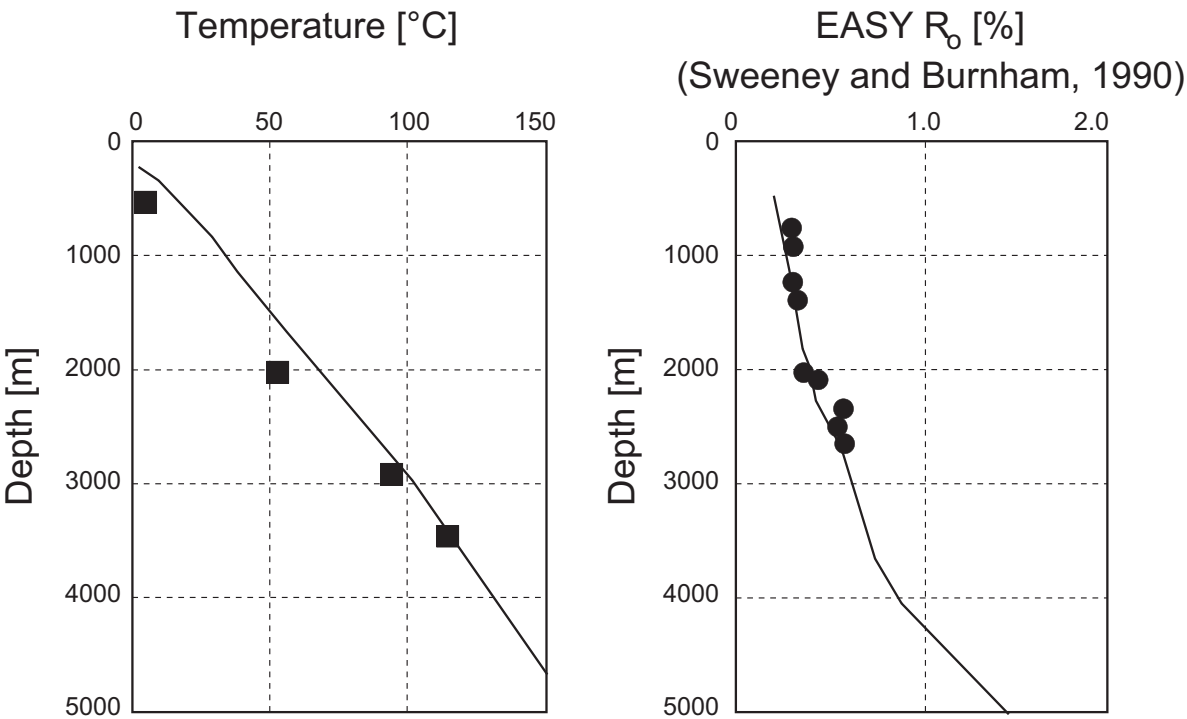


Fig.4. Calibration data (squares and circles) plotted against modelled vitrinite reflectance and temperature values (solid lines) for well 26/28-1.

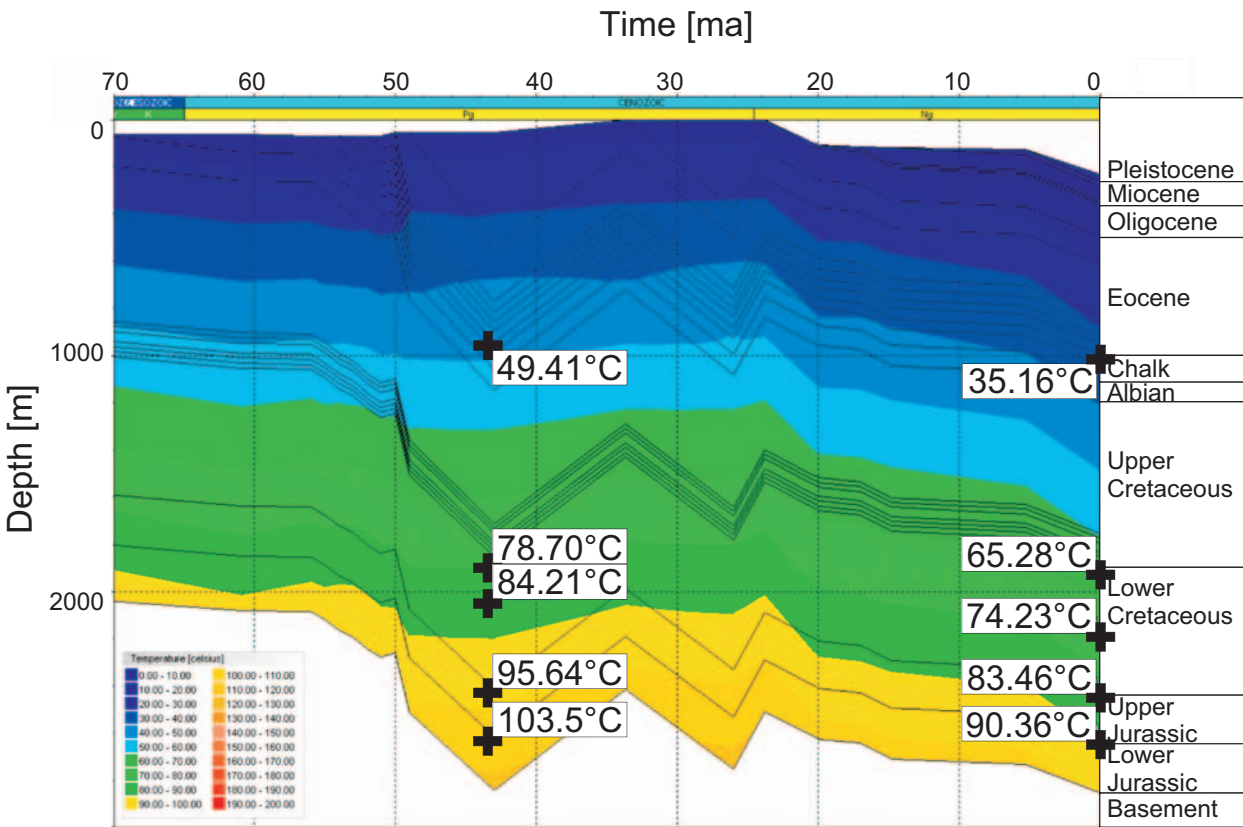


Fig.5. Temperature evolution through time in well 26/28-1. Marked temperatures for Eocene and present-day indicate that maximum temperatures (which closely match AFTA-temperatures as determined by McCulloch, 1993, for the same intervals) were reached during Eocene burial under the influence of the Iceland Plume.

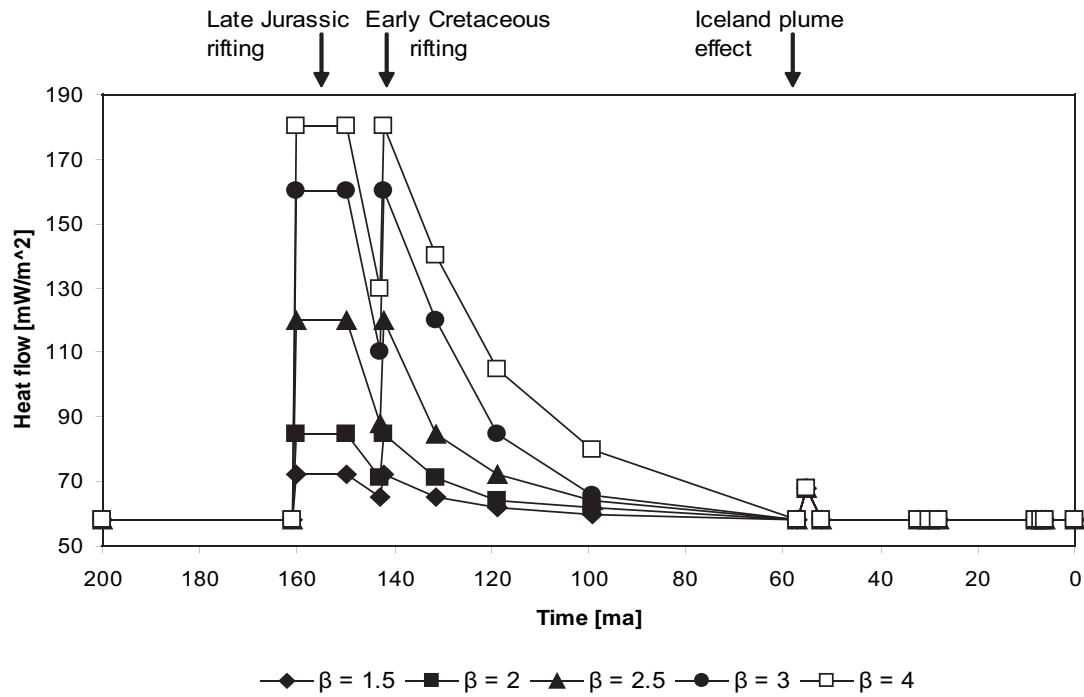


Fig.6. Heat flow based on rifting events and stretching magnitude as described by the stretching value  $\beta$ .

magnitude outlined above, and underline the importance of the Iceland Plume as far as the heat flow history of the Porcupine Basin is concerned.

Hydrocarbon generation kinetics

Basin analysis uses kinetic models to predict the extent of petroleum generation within potential source rocks from high-molecular weight kerogen (Pepper and Corvi, 1995; Schenk *et al.*, 1997). Predicting the composition of natural petroleum requires kinetic characterisation of both the primary reactions leading from kerogen to hydrocarbons and also the secondary transformations of the primary products into gases and other light hydrocarbons.

The kinetic parameters (activation energy distribution and a single frequency factor) for these reactions are determined from the pyrolysis of kerogen. Where source rock samples are absent, asphaltenes derived from oil samples can be used instead. Asphaltenes are organic macromolecular aggregates which bear close structural similarities to their precursor kerogens. Hence, kinetic information derived from oil asphaltenes can be used as an alternative to that derived from source rock kerogen (di Primio *et al.*, 2000). As no source rock material was available from wells drilled in the study area, asphaltenes from DST 1, well 26/28-1, were used for the determination of bulk hydrocarbon generation kinetics (Fig.7).

However, bulk kinetics are not able to predict

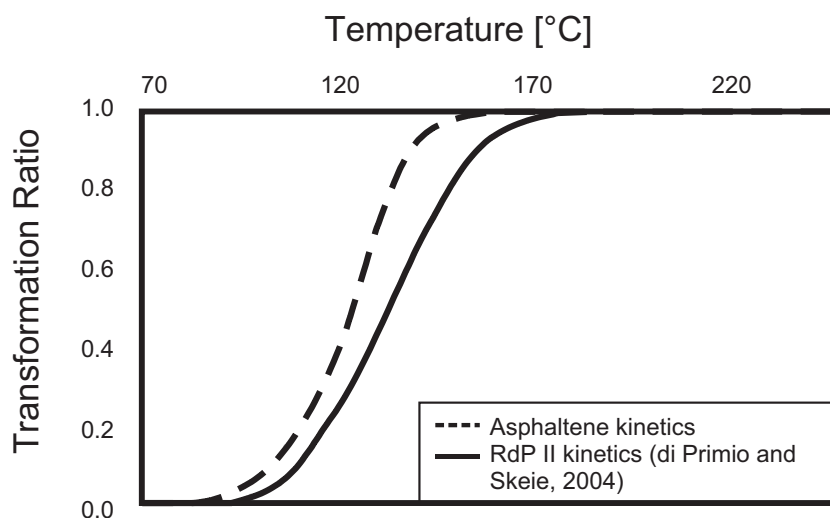
hydrocarbon compositions; they only describe the bulk generation of hydrocarbons from macromolecular organic matter by primary cracking. Compositional kinetic schemes allow a separate description of oil and gas generation as well as, in some cases, a compositional description of the phases generated. This makes it possible to take the phase behaviour and the differential migration of oil and gas phases into account during the simulation of petroleum migration, a prerequisite when attempting to reconstruct gas migration pathways.

Compositional kinetics (“RdP II”) developed by di Primio and Skeie (2004) for typical North Sea black oils divide the bulk fraction into nine components. Five of these characterise the gas composition (C1-C5), and four the high molecular weight fraction (C6, C7+ A, B, C). These models are compositionally compatible with standard PVT data and their predictions have been calibrated to natural fluid compositions.

The use of the di Primio and Skeie (2004) compositional kinetic model in this study is supported by the comparison of asphaltene kinetic and compositional kinetic predictions of kerogen transformation shown in Fig.7. Using a geologic heating rate of 3°C/Ma, predictions of onset and 50% transformation differ by only 5-10% respectively, well within the range of the observed kinetic variability of individual source rock organic facies (Tegelaar and Noble, 1993).



**Fig.7. Graph showing the variation of the Transformation Ratio with temperature for bulk (asphaltene) kinetics and for compositional RDP-II kinetics using a heating rate of 3°/Ma.**



## RESULTS

### Timing of Hydrocarbon Generation

Modelling results show that Jurassic and older source rocks in the basin are mature to overmature;  $R_o$  ranges from 0.7 to >4.7%, and present-day temperature from 95 to 260°C. Maturity values are low on the flanks of the basin. Fig.3 shows the calculated vitrinite reflectance for line *RE94*.

Cretaceous strata are immature to mature in the central part of the basin, and immature on the flanks. Vitrinite reflectance ranges between 0.3 and 4.6 %  $R_o$ , and present day temperatures between 40 and 240°C. Transformation Ratios (discussed below) show total conversion in the central part of the basin below 4,500 m.

The Tertiary sequence remains immature over the entire basin. Vitrinite reflectance reaches a maximum of 0.4 %  $R_o$ , and present day temperature ranges between 4 and 70°C.

The kinetics predict 100% conversion of kerogen for Jurassic material buried below 4,000 m and partial conversion for material above 4,000 m. But even in the shallowest parts of the basin, Jurassic kerogen has produced hydrocarbons. Generation of hydrocarbons starts in Cretaceous times for the Jurassic sequences shown in Fig. 8, and is related to the high heat flow occurring during the main rifting event. Generation continues up to the present day except during uplift in the Late Cretaceous and Paleocene. Generation rates increased in the Oligocene and Miocene due to the more rapid subsidence. Based on the compositional kinetic description used, around 70% of the total hydrocarbon potential has been realised by 45 million years before present.

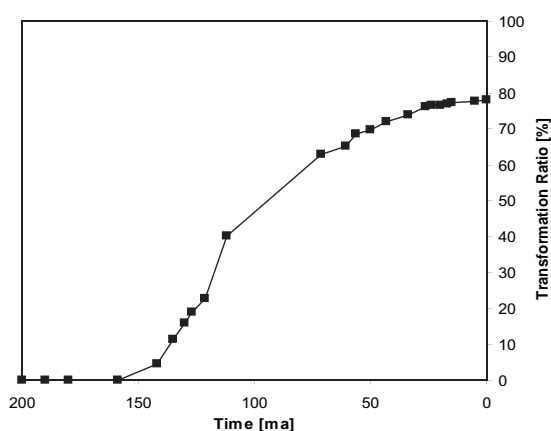
Based on the heat flow histories shown in Fig. 6, the present-day maturity of the base Cretaceous was calculated and is shown in Fig.9.

Fig.10 shows the implications of the burial and heat flow history modelled with respect to the timing

of hydrocarbon generation at various locations within the basin. In the basin centre (red dot and line on Fig.10), hydrocarbon generation from presumed Jurassic source units would mainly have been controlled by the development of the mid volcanic ridge, whereby associated significant stretching and enhanced heat flow would already have exhausted any source potential by Early Cretaceous times. Along the flanks of the basin (green dot and line on Fig.10), the Early Cretaceous rifting and high heat flow was still strong enough to mature the Jurassic source rocks to a level well within the gas window ( $R_o > 2\%$ ). During Tertiary burial, some gas derived from cracking of residual oil may have been mobilised in this area. The margins of the basin (blue dot and line on Fig.10, situated to the SW of the *Connemara* discovery well 26/28-1) represent the best locations for recent to ongoing hydrocarbon generation in the basin, whereby source rock maturation occurred continuously throughout the burial history and is still proceeding today.

### Migration

For the three regional seismic lines *RE25*, *RE88* and *RE94*, modelled hydrocarbon flow was simulated across the basin in the following time steps: 205, 180, 142, 121, 112, 71.3, 60.9, 56, 54.8, 43, 33.7, 23.8, 5.3 Ma and present day. Migration of hydrocarbons starts when Jurassic organic matter enters the oil window during the Early Cretaceous. In the central part of the basin, early generated Jurassic gas migrates mainly vertically through to the surface; whereas towards the end of the Cretaceous, this area generates liquid hydrocarbons which also start to migrate vertically. Phase separation, predicted by the use of compositional kinetics, is observed over a depth range of 1,000-1,500 m throughout the entire basin. During Albian times, oil and gas accumulates in the Aptian sandstone interval which is sealed by the Late Cretaceous marl. Some accumulations are modelled



**Fig.8. Calculated transformation ratio for the di Primio and Skeie (2004) compositional kinetics.**

to exist in the Albian carrier system up to present day. However, it should be noted that the structural traps in the 2D model may be artefacts due to the absence of the third dimension. Hydrocarbons may also migrate through the marl at locations where the hydrocarbon column height leads to capillary failure of the cap rock and into the Tertiary, where the Paleocene sandstone layers are a major carrier system. If continuous throughout the basin, the Albian sandstones seem to be a main migration pathway due to their relatively high porosity (about 25-30% based on well data).

Migration is more active in the northern part of the basin during the Eocene due to additional loading and enhanced generation following burial under the prograding delta front. Migration remains mainly vertical, except for lateral migration along the Albian and Paleocene layers. The end of the Eocene is marked by an erosional event followed by renewed subsidence during Oligocene times, during which migration occurs following the same general pattern.

Intrusions of Miocene age in Cretaceous units will locally generate some hydrocarbons, which migrate into the Albian interval and from there into traps or laterally out of the model. Later in the Miocene, migration still remains vertical with some focussing of hydrocarbon flow through Miocene slump structures and polygonally faulted sediments (see below). The Late Miocene and Early Pliocene are marked by strong subsidence in the southern part of the basin, concentrating generation and migration of hydrocarbons into that area, again with mainly vertical migration.

Migration patterns in the high resolution lines modelled are discussed in the following paragraphs.

#### **Line PORC97-12**

Stratigraphic detail was provided by the seismic interpretation of line PORC97-12. The line terminates

in the basin centre and crosses the Belgica mound province. The presence of mound SP46 on the seismic line allows us to assess whether there is a link between surface leakage and mound occurrence. Fig.11 shows the simulation results using the conceptual model input parameters, petroleum properties and respective phase behaviour as defined by the compositional kinetic model. Vectors for oil migration are shown in green; vectors representing gas migration are marked in red.

In this section, hydrocarbon generation started in the Early Cretaceous from the Jurassic source rock. The source rock is overmature in the centre of the basin at the present day (see above). Migration towards the eastern flank of the basin started in the Early Cretaceous. Shaly and muddy sequences seal the Albian sandstones which act as a high permeability migration pathway. These Aptian carriers pinch out on the basement on the eastern flank and may form a stratigraphic trap. The Late Cretaceous is marked by the deposition of chalk with a more-or-less constant thickness. Tertiary sequences consist mainly of muddy lithologies whose thickness decreases towards the eastern flank. The influence of the Paleocene Iceland Plume and of alpidic orogenesis led to basin uplift and to the deposition of the Paleocene marine sand from the shoreline above the basement high on the eastern flank to the basin centre. Thermal subsidence led to rapid burial and the development of deep marine environments, characterised by the deposition of shaly, silty sequences. These lithologies have not been confirmed by drilling and are assigned according to the conceptual model and observations made on wells in the Porcupine Basin.

The predicted petroleum composition is characterised by a high gas content due to the relatively elevated maturity of the source rocks. Such gas-rich fluids quickly become saturated during upward migration and separate into oil and gas. In

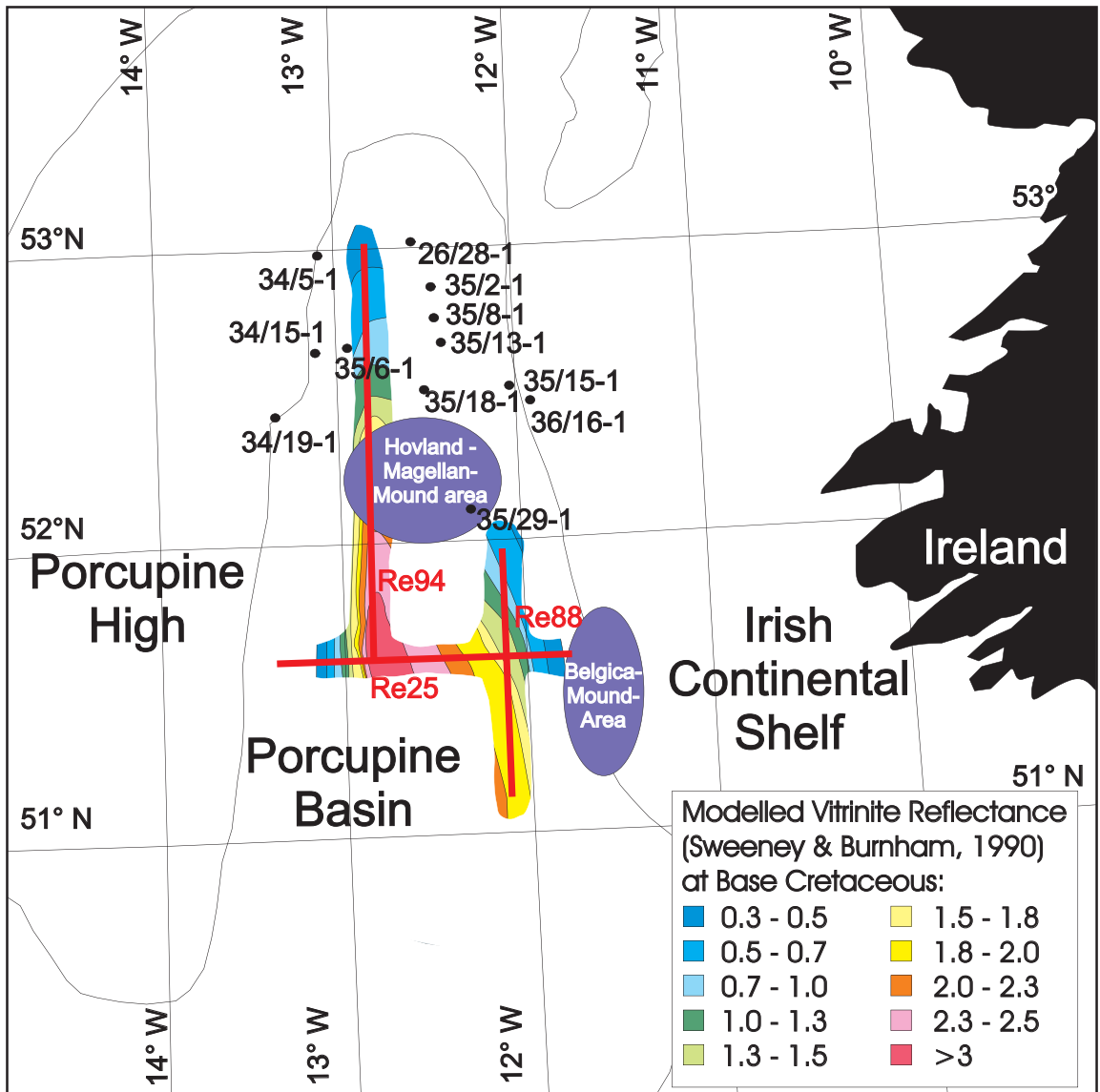


**Fig.9.** Present-day thermal maturity of the base Cretaceous in the vicinity of the modelled lines. Calculations based on the heat flow history of the basin. Vitrinite reflectance was calculated using the vitrinite kinetics developed by Sweeney and Burnham (1990).

the modelling software used, the phase behaviour of the fluids is calculated using the Soave-Redlich-Kwong equation of state (Soave, 1972). The difference in migration rates and fluid mobility between oil and gas increases with decreasing pressure. In the upper 4,000 m of the section studied, separate-phase gas migration is the dominant process. Migration pathways are Albian and Paleocene sandstone intervals. Hydrocarbons are trapped in the pinch-out of the Albian carrier on the eastern basement high. The low capillary entry pressures of the thin Late Albian shales, Late Cretaceous chinks and weakly consolidated Tertiary mudstones direct hydrocarbon flow into the Paleocene carrier system. A reactivation of the faults bounding the Jurassic rotated block during the Early Tertiary tectonic stress regime might also open migration conduits but is not necessary to explain the leakage into the Paleocene sequence.

Hydrocarbons flow along the highly permeable Paleocene sandstones towards the eastern margin of the basin. The Paleocene layer pinches out on the basement structural high. The overlying shaly and silty mudstones are only weakly consolidated and allow seepage of hydrocarbons towards the seafloor. As this pinch-out is located below the Belgica mound province, a link between mound occurrence and hydrocarbon seepage is feasible.

As no well control was available in the Belgica region, it was impossible to constrain the model definition (lithologies used, stratigraphy, etc.) as well as its predictions regarding sediment porosities, permeabilities or capillary entry pressures. Accordingly, the results concerning focussing of hydrocarbon leakage remain questionable. The main uncertainty is linked to the sediment properties, as the permeability contrast between carrier and cap rock

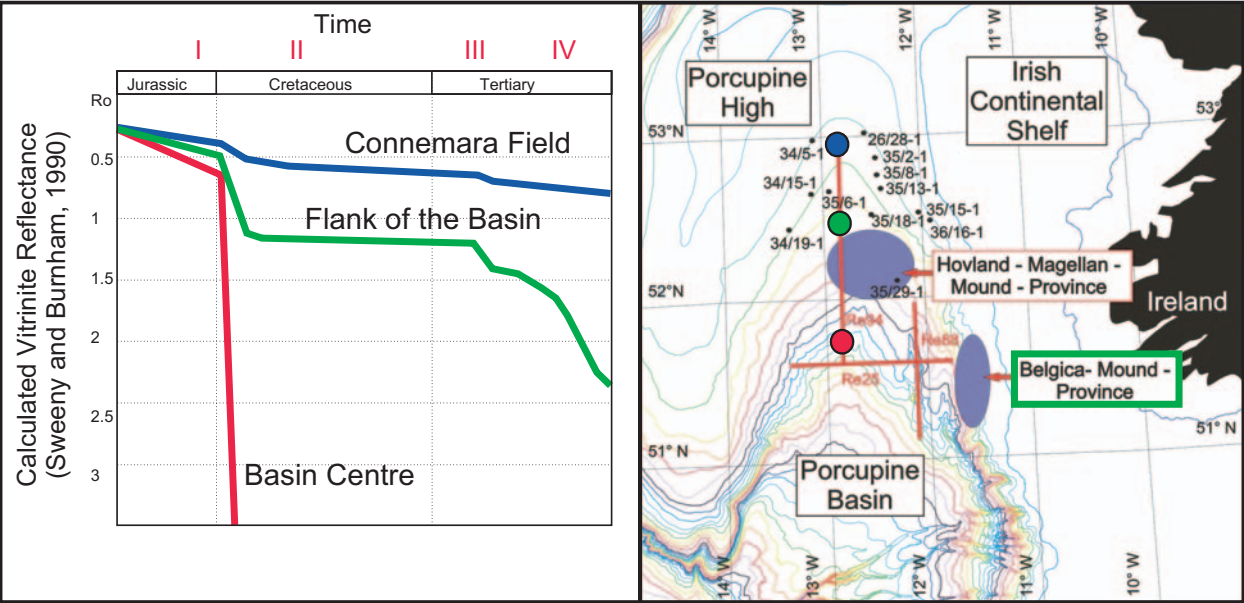


**Fig.10. Evolution of the maturity of a postulated Upper Jurassic source rock at three locations in the basin (blue: Connemara field; green: flank of the basin; red: basin centre).**

is the main controlling element for hydrocarbon leakage. In order to test our predictions in the Belgica area in this respect, a study area with good well control and known gas leakage was used as a test case.

**Connemara Line CS2**

Connemara line CS2 runs through well 26/28-1 and shows evidence of gas chimneys and pockmarks on the seafloor.

The basin geometry is controlled by the structural highs consisting of rotated Jurassic fault blocks and older sequences. The sedimentary sequence in well 26/28-1 starts with sediments of Devonian age overlain by Carboniferous coaly sequences. An unconformity follows with sedimentation starting again in the Middle Jurassic and continuing to present. Albian sandstones reach a maximum thickness of about 200 m at the basin centre. This sequence is overlain by thin shales (maximum thickness about 50 m), by Late Cretaceous chalk deposits and then Tertiary shaly and sandy sequences.

The Jurassic source rocks remain immature in this cross-section due to shallow burial. But, as observed in the results from lines RE94, RE25, RE88 and PORC97-12, the hydrocarbon kitchen is located further towards the basin centre which is outside of line CS2. To analyse the location and magnitude of preferred leakage sites from reservoirs, Jurassic source properties were also assigned to the deeper Carboniferous sequence, giving it an adequate, albeit hypothetical, potential and maturity to generate hydrocarbons. Obviously, a 3D model which included

the actual source sequences of the Connemara area would have been the best option; but as such information was not available, the use of a local deeper kitchen area within the 2D section was deemed adequate for the purposes of this study. It is important to note that the purpose of the Connemara simulations was to check whether the cap rock lithologic definitions used in the regional and high-resolution 2D studies were appropriate.

The modelled petroleum composition is based on RdPII compositional kinetics. Fluids generated by the source rocks migrate vertically into the Jurassic carrier beds and then laterally until they reach the structurally highest position (Fig. 12). As the sandstones are sealed by overlying Cretaceous sediments as well as by juxtaposition across the boundary faults of the rotated fault blocks, hydrocarbons accumulate in these structures. One of these structural traps was drilled in well 26/28-1, and the correlation of predicted and discovered hydrocarbons supports the modelling parameters used. Leakage occurs when the hydrocarbon column in the accumulations exceeds the capillary entry pressure of the cap rock lithologies. The leaking hydrocarbons experience decreasing pressure and temperature during vertical migration, leading to phase separation and the coexistence of migrating oil and gas phases. The location of the main leakage sites directly above the structural closures in the model coincides with the location of the observed gas chimneys. Modelled focussed seepage through to the seafloor also indicates the possibility of pockmarks.



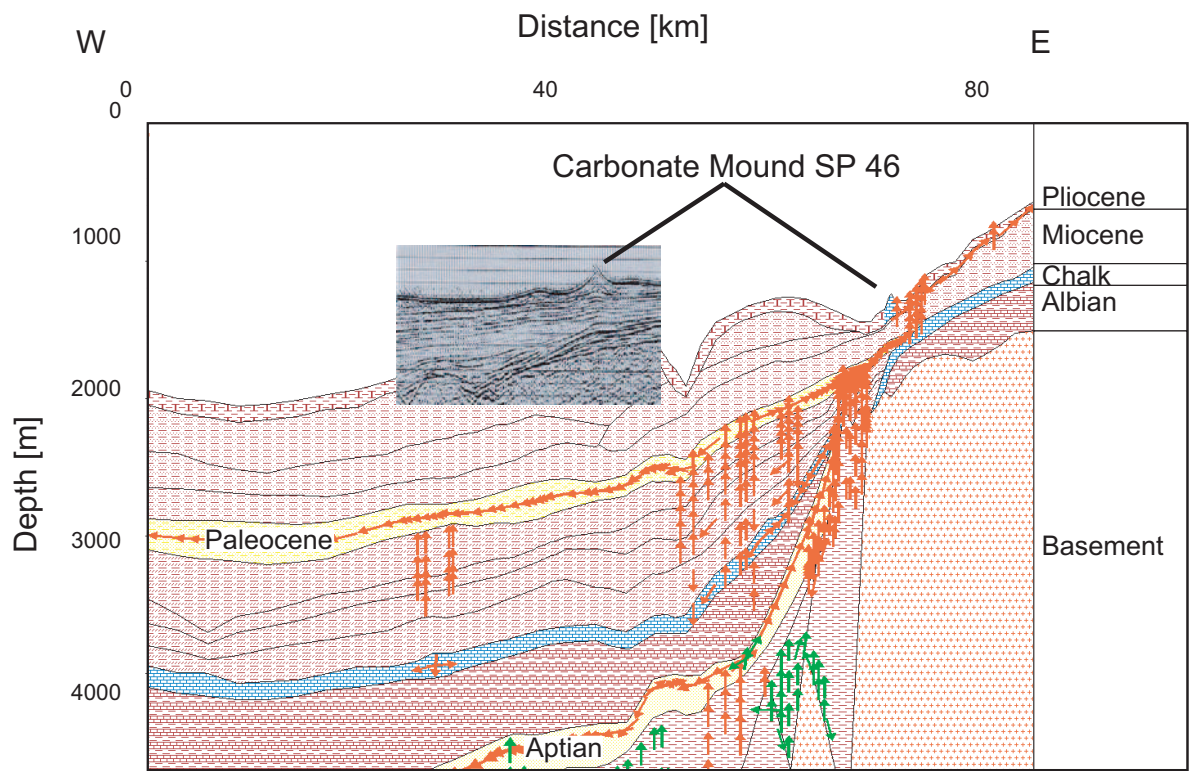


Fig.11. Modelled migration of gas (red vectors) and oil (green vectors) at present day along Aptian and Paleocene sandstone layers (yellow) on profile PORC97-12 towards the Carbonate Mound SP46.

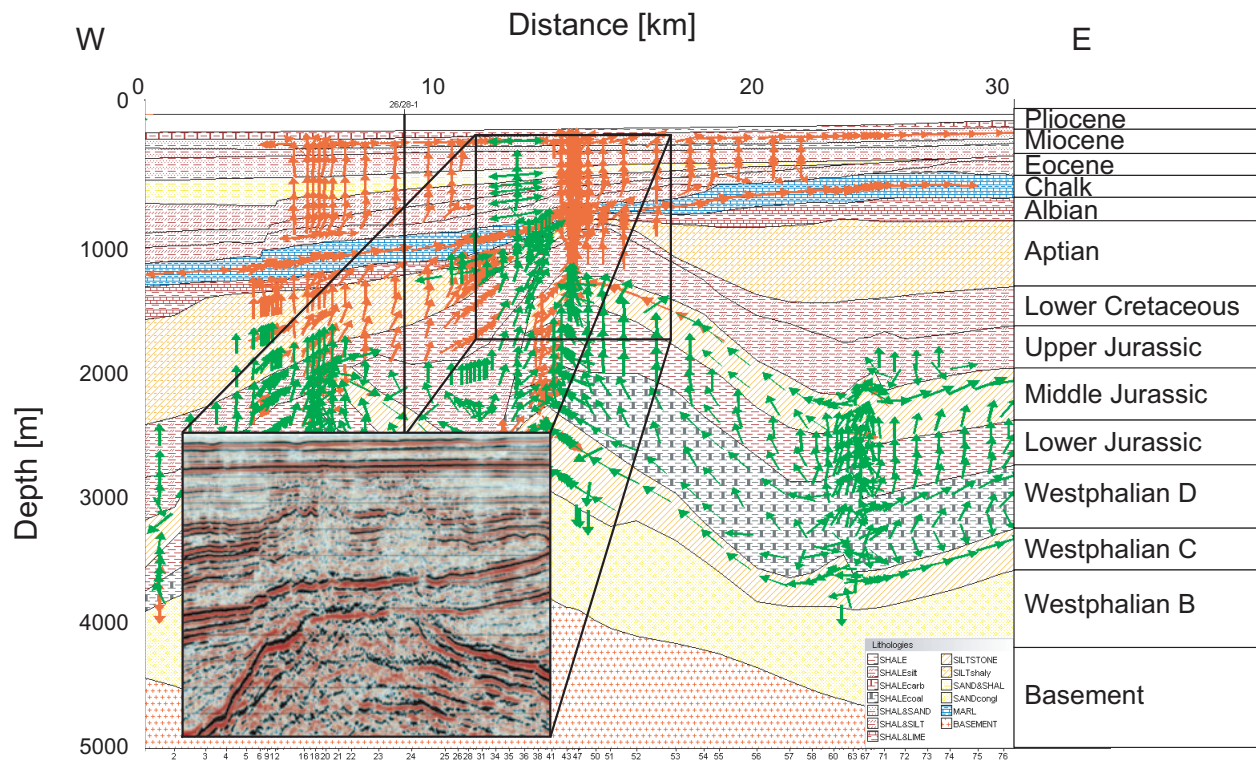


Fig.12. Profile CS2 through the Connemara field showing well 26/28-1 and modelled gas (red vectors) and oil (green vectors) flow directions.

The properties of the boundary faults were modelled as open (permeable) and closed (impermeable) faults in sensitivity runs. Fault properties had no effect on the migration pathways, but the volumes of migrating hydrocarbons were slightly different. Therefore, capillary failure of the cap rock was again the main controlling factor for hydrocarbon migration. The modelling results also indicate that fracturing of the cap rock lithologies due to the build-up of overpressure need not be invoked in order to explain the preferred leakage sites. Available pressure data from the wells studied also indicate the prevalence of near-hydrostatic conditions in the reservoir units, again excluding cap rock fracturing as a necessary leakage mechanism.

The *Connemara* section is also an ideal location for assessing the compositional predictions of the kinetic models used. Predicted compositions of accumulations can be compared to the above-described physical oil samples. Predicted API-values of 35° and a methane content of below 18% indicate the occurrence of a black oil. Modelled oil compositions fit well with observations by Scotchman (2001). Measured API gravities ranged between 30 and 36° for the *Connemara* field. MacDonald *et al.* (1987) reported 195 million barrels of light, waxy oil in place and reserves of 40-80 MM brl oil. The model predictions fit these observations.

As the modelled hydrocarbon accumulations, gas chimneys and pockmarks corroborate the observations, we infer that the lithologic descriptions and compaction behaviour correctly reproduce the natural system; and that extrapolation of the same lithologic properties to shallower settings such as the Belgica region is therefore valid. We also assume that the modelled migration pathways in the line *PORC97-12* for the Belgica mound province correctly describe the natural processes. Clearly, focussing and accumulation of the migrating hydrocarbons to the site of leakage is a prerequisite for the development of a discrete leakage site. In 2D, the assumption is made that the cross-section modelled in fact represents such a situation.

### Hovland-Magellan mound province

#### 2D modelling

The Hovland-Magellan mound province is located in the central part of line *RE94*. Due to the scale and location of the line, no mounds can be observed on the seismic profile. The set-up for the line is the same as that described before. Migration pathways are the Aptian and Paleocene sandstones which direct hydrocarbon flow out of the modelled line (Fig.13). The dominant pattern is again vertical migration controlled by capillary leakage and lateral flow in the high-permeability units. Only minor focussing of

hydrocarbon leakage is predicted by the model at the location of the Aptian carrier system pinch-out. This focussing, however, does not lead to hydrocarbons reaching the surface in the model.

Early Tertiary deltaic sequences, slump structures and Late Tertiary contourites have been proposed to focus hydrocarbons towards the mound area (McDonnell, 2001). Incorporation of these structures into the model, as shown in Fig.13, did not result in any obvious focussing of hydrocarbons. The lack of focus in the modelled flow patterns is probably a problem of seismic resolution and also of two-dimensional modelling, as the structure and topography of layers direct flow laterally and can influence the fluid flow in 3D. A 3D seismic survey was not available for this study. However, maps of the Oligocene (C30), Miocene (C20), mid-Miocene and base-Pliocene (C10), based on the *MS81* survey and mapped in the framework of the STRATAGEM project\* were available. These maps were used for drainage area calculations based on the present-day topography of the layers to analyse possible flow patterns in this part of the Porcupine Basin.

#### Drainage area modelling

Using flow path modelling, fluid flow is modelled as a purely geometrical problem (Hantschel *et al.*, 2000; Sylta, 1991). The driving force for migration is buoyancy; assuming that a capillary pressure threshold is exceeded the entire carrier rock can be treated as flow conducting. The map is subdivided into drainage areas, and the petroleum in each drainage area is moved to its proper trap assuming that migration occurs instantaneously relative to the geologic time scale and also that physical interactions during migration are negligible. Such methods are also known as ray tracing, map-based, surface-based or 2.5D models (Sylta, 1991). In this case, all of the petroleum in one drainage area begins to migrate following the flowpaths towards the reservoir, which is mapped as a closure defined by the topographic position in relation to the surrounding drainage area. Spilling takes place when a trap is completely filled. Possible spill flowpaths into the bordering drainage areas can be calculated from the map structure.

The calculation of the drainage areas of the four maps provides the drainage area boundaries and closures based on the present-day topography. The closures could be areas of possible hydrocarbon accumulations. Hydrocarbon leakage would be expected to occur above the closures, since these represent probable sites of enhanced hydrocarbon column height. If mound growth is hydrocarbon-

\* Stratigraphic Development of the Glaciated European Margin, Project Reference: EVK3-CT-1999-00011.

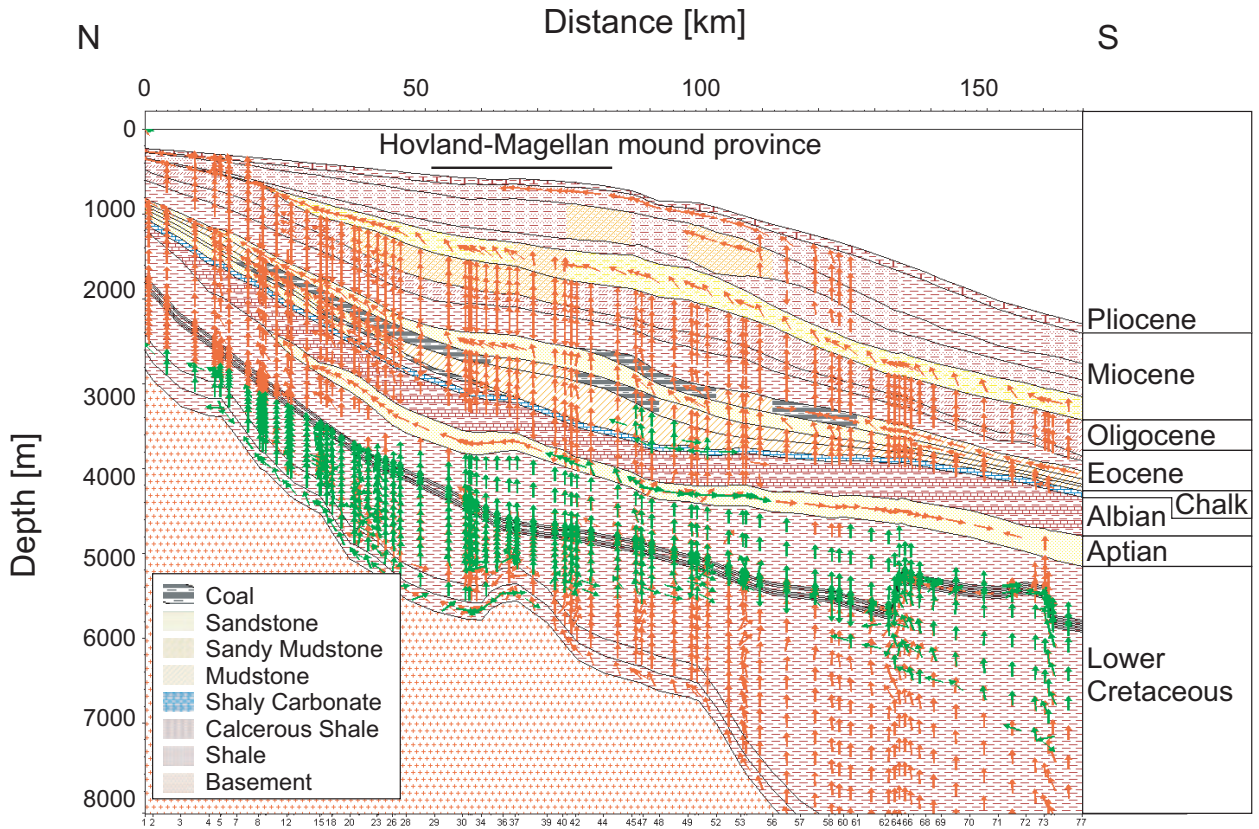


**Fig. 13. Modelled gas flow (red vectors) and oil flow (green vectors) at present day on profile RE94 in the Hovland-Magellan mound area.**

related, one would expect mound locations to be geographically associated with these closures.

Fig. 14 shows the superposition of all mapped boundaries and closures as well as the positions of buried and surface mounds in the Hovland-Magellan area. Fig. 14 shows a high degree of correlation of mound location and closures for the surface mounds. The correlation is limited due to the poor resolution of the maps and the limited areal distribution; it is best for the central parts of the maps, where the calculation of the drainage areas is not influenced by the map boundaries, i.e. where map quality is best.

For the buried mounds, no coincidence of mounds and closures was observed. However, mound locations roughly display a NE-SW trend which runs parallel to the calculated drainage area boundaries. This could indicate a link to a deeper structure which could be a structural or stratigraphic feature such as observed beneath the Belgica mound province.

## DISCUSSION

The results presented above indicate that a coincidence between carbonate mound occurrence and present or palaeo hydrocarbon leakage is likely for each of the areas studied. However, the methods used for arriving at this interpretation, namely 2D modelling and map-based modelling, are not optimal. Especially when

modelling hydrocarbon migration, it is obvious that a process which is clearly dependant on lithologic variations in three dimensions can only roughly be approximated using 2D methods. We chose to use 2D modelling in this study due to the limitations imposed by the data available, which consisted of interpreted 2D seismic lines and only selected maps based on 2D interpretation. Nevertheless, the lines modelled were carefully picked from the available database so as best to represent the Porcupine Basin. We believe 2D basin modelling is a valid tool to use when addressing the processes which control petroleum migration, i.e. whether migration focussing by faults, stratigraphic pinch-outs or structural closures is required, or whether capillary entry pressures of cap rock lithologies control the sites of leakage.

We used this approach in the determination of leakage sites in the sections studied. Stratigraphic pinch-out of carrier lithologies was the main factor controlling sites of enhanced hydrocarbon leakage in the Belgica area. The most sensitive assumptions made in this part of the study were the definitions of the lithologies of the individual model events (i.e. carriers and cap rocks), as well-control in the area was not available. Extrapolation of lithologies from the northern part of the basin into the Belgica area led to a model which predicted the leakage of hydrocarbons in the direct vicinity of the actual mound location.



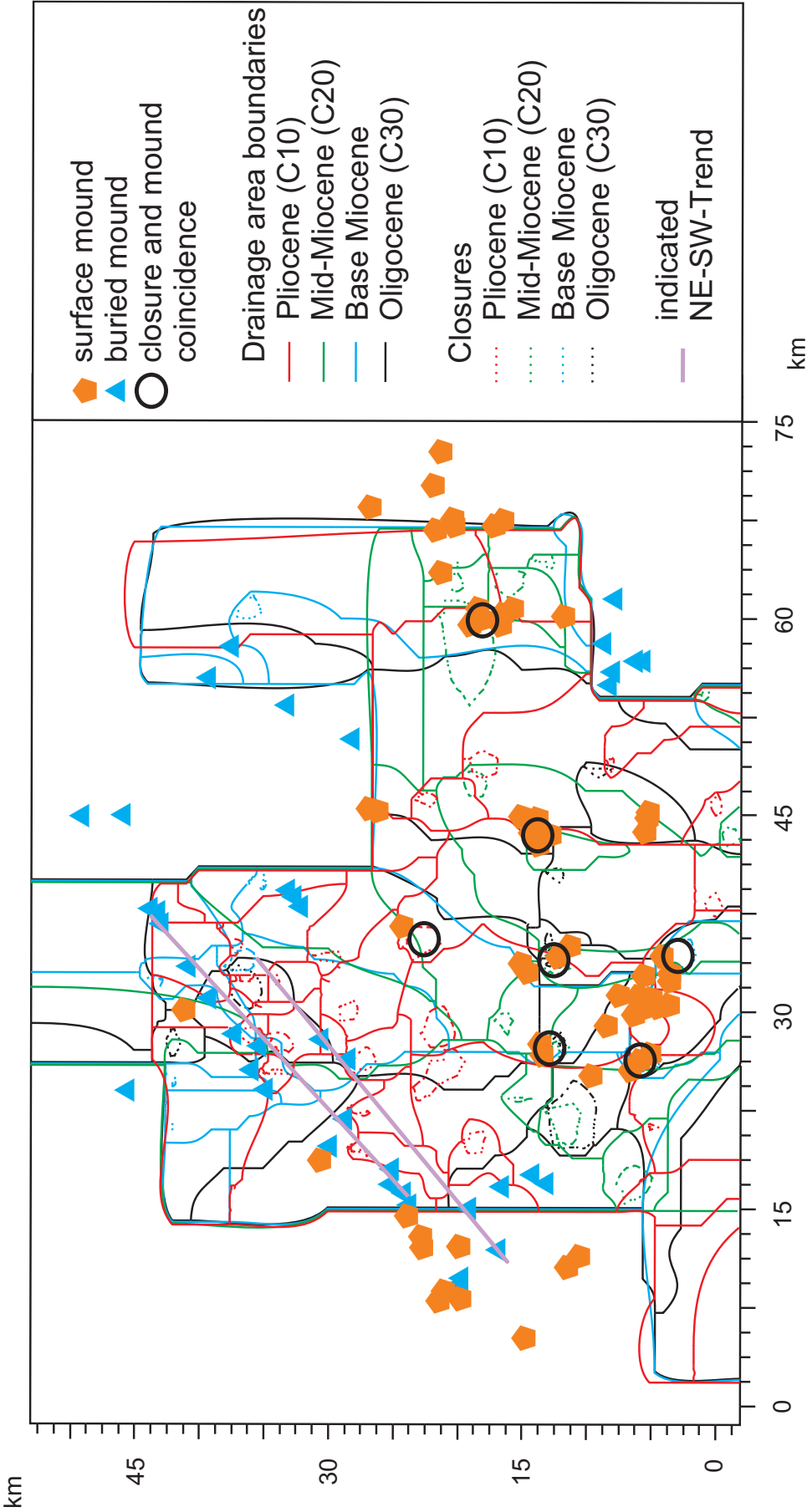


Fig. 14. Results from the drainage area analysis: coincidence of surface mounds and closures are marked by black circles and the trend seen in the buried mounds is marked by the violet lines.



Although the three dimensional situation may not correspond to our 2D model, the fact that the strike of the major fault systems on the SE flank of the Porcupine Basin is parallel to the strike of the mound lineations in the Belgica area (de Mol *et al.*, 2002; McCann *et al.*, 1995) indicates that stratigraphic pinch-out of carriers on this faulted rift shoulder is a likely pathway linking hydrocarbon leakage and mound location.

In the *Connemara* area, the same event characterisation was used as in the Belgica area. Observed gas chimneys were also reproduced by the model, despite the relatively large differences in the respective burial histories. In the *Connemara* area where well control was readily available, the main model uncertainties were related to the correct simulation of source rock maturation.

In the Hovland-Magellan area, there were no indications of stratigraphic, structural or fault-controlled focussing of the predominantly vertical hydrocarbon leakage pattern. In this case, it was obvious that a simple 2D approach was not appropriate. Drainage and closure area modelling using maps of the main upper Tertiary reflectors indicated a high degree of correlation between closures on the maps and surface carbonate mounds. While this observation is only valid for the present day, it suggests a causal relationship.

In all cases studied, the main control on sites of hydrocarbon leakage was the presence of a hydrocarbon column, and the subsequent capillary failure of the cap rock lithology. Faults were not necessary to reproduce sites of leakage in the cases studied. Hence, our results do not support the interpretation presented by Hovland *et al.* (1994).

The question remains why carbonate mounds only occur in the Hovland-Magellan and Belgica areas, and yet no mounds are found in the *Connemara* area, where leakage occurs. Clearly the availability of leaking hydrocarbons by itself will not result in carbonate mound formation, but a combination of factors is most probably required. Metabolism of hydrocarbons by bacteria at the seafloor can result in the formation of carbonate hardgrounds (Hinrichs and Boetius, 2002), which present optimal colonisation sites for deep-water corals. However, coral growth also depends on other factors including: the presence of water currents providing suspended nutrients; the correct temperature conditions for optimal growth; and low sedimentation rates so that the growing mounds are not buried.

These additional factors appear to occur in the Hovland-Magellan and Belgica areas of the Porcupine Basin; however, the primary control, namely the availability of suitable colonisation sites, seems to be controlled by hydrocarbon leakage.

## CONCLUSIONS

The aim of this study was to investigate whether there is a link between hydrocarbon leakage and the occurrence of carbonate mounds on the seafloor.

Modelling of hydrocarbon generation and migration indicates that the main Jurassic source rocks are mature to overmature throughout the studied part of the Porcupine Basin. Hydrocarbon generation started in Late Cretaceous times for the deepest Jurassic sequences, and is still ongoing today along the flanks of the basin. Based on the compositional kinetic model used, the Upper Jurassic source rock generates undersaturated black oil while in the oil window, with gas condensate dominating at higher maturities. Phase separation was modelled to occur during migration at depth ranges between 1,000 and 4,000m (depending on the fluids composition). Upon phase separation, migration of the free gas phase dominates over that of the oil, such that gas is the main migrating fluid in the shallower intervals. Migration is mainly vertical, and only Aptian and Tertiary deltaic intervals direct hydrocarbon flow out of the basin. Modelling predictions over the entire basin indicate gas breaking through to the seafloor.

On seismic line *PORC97-12*, representing the geology in the Belgica mound province, the model predicts a significant focussing of gas migration towards the mounds, beneath which a pinch-out of Cretaceous and Tertiary layers is observed.

In the 2D studies of the Hovland-Magellan mound province, no obvious focussing of hydrocarbon leakage towards mounds was observed. This lack of focussing could reflect either lack of sufficient stratigraphic detail in the model, or the inadequacy of using a 2D model for the simulation of an essentially 3D process. Using drainage area analysis (map-based flow modelling), the locations of surface mounds correlated well with mapped closures in the Oligocene (C30), Miocene (C20), mid-Miocene and base Pliocene (C10), indicating the likelihood of a link between preferred sites of fluid leakage and mound location. The locations of buried mounds in the area track mapped drainage area boundaries, pointing towards a possible link to a deeper structural feature. Further seismic investigation is needed to confirm this observation.

The results of this study indicate that carbonate mounds, in addition to pockmarks and mud volcanoes, may be surface expressions of an underlying active petroleum system.

## ACKNOWLEDGEMENTS

This work was carried out as part of the Geomound Project supported by the European Commission under

the Fifth Framework Programme (EU Contract N° EVK3-CT-1999-00016). The authors would like to thank all Geomound colleagues and the technical staff of FZJ and GFZ. Thanks are also due to JPG referees S. Burley and M. Erdmann whose reviews significantly improved the manuscript. Comments and suggestions by H. Poelchau, C. Zwach and an anonymous reviewer on a previous version of this paper are also gratefully acknowledged.

## REFERENCES

- BATHURST, R.G.C., 1975. Diagenetic fabrics in some British Dinantian limestones. In: *Sedimentary rocks; concepts and history*. Dowden Hutchinson & Ross Inc., Stroudsburg, Pa., 288-314.
- BUTTERWORTH, P., HOLBA, A., HERTIG, S., HUGHES, W. and ATKINSON, C., 1999. Jurassic non-marine source rocks and oils of the Porcupine Basin and other North Atlantic margin basins. In: Fleet, A.J. and Boldy, S.A.R. (Eds), *Petroleum geology of Northwest Europe*. Proceedings of the 5th Conference, *Geological Society of London*, 471-486.
- CLIFT, P.D., CARTER, A. and HURFORD, A.J., 1998. The erosional and uplift history of NE Atlantic passive margins: constraints on a passing plume. *Journal of the Geological Society, London*, **155**, 787-800.
- CROKER, P.F. and SHANNON, P.M., 1987. The evolution and hydrocarbon prospectivity of the Porcupine Basin, Offshore Ireland. In: GLENNIE, K. (Ed), *Petroleum Geology of North West Europe - Proceedings of the 3rd Conference on Petroleum Geology of North West Europe*, October 1986. Graham & Trotman, 633-642.
- CROKER, P.F. and SHANNON, P.M., 1995. The petroleum geology of Ireland's offshore basins: intro. In: Croker, P.F. and Shannon, P.M. (Eds), *The petroleum geology of Ireland's offshore basins*. *Geol. Soc. Lond., Spec. Pub.* **93**, 1-8.
- DE MOL, B., VAN RENSBERGEN, P., PILLEN, S., VAN HERREWEGHE, K., VAN ROOIJ, D., MCDONNELL, A., HUVENNE, V., IVANOV, M., SWENNEN, R. and HENRIET, J.P., 2002. Large deep-water coral banks in the Porcupine Basin, southwest of Ireland. *Marine Geology*, **188**, 193-231.
- DI PRIMIO, R., HORSFIELD, B. and GUZMAN-VEGA, M.A., 2000. Determining the temperature of petroleum formation from the kinetic properties of petroleum asphaltenes. *Nature*, **406**, 173-176.
- DI PRIMIO, R. and SKEIE, J.E., 2004. Development of a compositional kinetic model for hydrocarbon generation and phase equilibria modelling: A case study from Snorre Field, Norwegian North Sea. In: J.M., C., ENGLAND, W.A. and LARTER, S.R. (Eds), *Understanding Petroleum Reservoirs: Towards an Integrated Reservoir Engineering and Geochemical Approach*. *Geol. Soc. Lond., Spec. Pub.* **237**, 157-174.
- EDWARDS, J.W.F., 2002. Development of the Hatton - Rockall Basin, North - East Atlantic Ocean. *Marine and Petroleum Geology*, **19**, 193-202.
- FARROW, G.E. and DURANT, G.P., 1985. Carbonate-basaltic sediments from Cobb Seamount, Northeast Pacific; zonation, bioerosion and petrology. *Marine Geology*, **65**, 73-102.
- FREDERIKSEN, R., JENSEN, A. and WESTERBERG, H., 1992. The distribution of the Scleractinian Coral *Lophelia pertusa* around the Faroe Islands and the relation to internal tidal mixing. *Sarsia*, **77**, 157-171.
- GRADSTEIN, F.M. and OGG, J., 1996. A Phanerozoic time-scale. *Episodes*, **19**, 3-5.
- GRASSLE, J.F., 1985. Hydrothermal vent animals; distribution and biology. *Science*, **229**, 713-717.
- HANTSCH, T., KAUERAUF, A.I. and WYGRALA, B., 2000. Finite element analysis and ray tracing modeling of petroleum migration. *Marine and Petrol. Geol.*, **17**, 815-820.
- HENRIET, J.P., DE, M.B., VANNESTE, M., HUVENNE, V. and VAN, R.D., 2001. Carbonate mounds and slope failures in the Porcupine Basin; a development model involving fluid venting. In: Shannon, P.M., Houghton, P.D.W. & Corcoran, D.V. (Eds.), *The petroleum exploration of Ireland's offshore basins*. *Geol. Soc. Lond., Spec. Pub.*, **188**, 375-383.
- HENRIET, J.P., MOL, B.D., PILLEN, S., VANNESTE, M., ROOIJ, D.V. and VERSTEEG, W., 1998. Gas hydrates may help build reefs. *Nature*, **391**, 648-649.
- HENRIET, J.P., VAN, R.D., HUVENNE, V., DE, M.B. and GUIDARD, S., 2003. Mounds and sediment drift in the Porcupine Basin, west of Ireland. *European margin sediment dynamics; side-scan sonar and seismic images*. Springer-Verlag.
- HINRICHS, K.U. and BOETIUS, A., 2002. The Anaerobic Oxidation of Methane: New Insights in Microbial Ecology and Biogeochemistry. In: G. Wefer, D. Billet, D. Hebbeln, B.B. Jørgensen, M. Schlüter, T. van Weering (Eds), *Ocean Margin Systems*. Springer-Verlag, pp. 457-477.
- HOVLAND, M., 1990. Do carbonate reefs form due to fluid seepage? *Terra Nova*, **2**, 8-18.
- HOVLAND, M., CROKER, P.F. and MARTIN, M., 1994. Fault-associated seabed mounds (carbonate knolls?) off western Ireland and north-west Australia. *Marine and Petroleum Geology*, **11**, 232-246.
- HUVENNE, V.A.I., CROKER, P.F. and HENRIET, J.P., 2002. A refreshing 3D view of an ancient sediment collapse and slope failure. *Terra Nova*, **14**, 33-40.
- HUVENNE, V.A.I., DE MOL, B. and HENRIET, J.-P., 2003. A 3D seismic study of the morphology and spatial distribution of buried coral banks in the Porcupine Basin, SW of Ireland. *Marine Geology*, **198**, 5-25.
- JAMES, N.P., 1997. The cool-water carbonate depositional realm. In: James, N.P. and Clarke, J.A.D. (Eds), *Cool-water carbonates*. *SEPM Spec. Pub.*, **56**, 1-20.
- LUNDIN, E. and DORÉ, A.G., 2002. Mid-Cenozoic post-breakup deformation in the 'passive' margins bordering the Norwegian-Greenland Sea. *Marine and Petroleum Geology*, **19**, 79-93.
- MACDONALD, H., ALLAN, P.M. and LOVELL, J.P.B., 1987. Geology of oil accumulation in Block 26/28, Porcupine Basin, Offshore Ireland. In: BROOKS, J. and GLENNIE, K. (Eds), *Petroleum Geology of North West Europe*. Graham & Trotman, 643-651.
- MACLENNAN, J., MCKENZIE, D. and GRONVÖLD, K., 2001. Plume-driven upwelling under central Iceland. *Earth and Planetary Science Letters*, **194**, 67-82.
- MCCANN, T., SHANNON, P.M. and MOORE, J.G., 1995. Fault patterns in the Cretaceous and Tertiary (end syn-rift, thermal subsidence) succession of the Porcupine Basin, offshore Ireland. *Journal of Structural Geology*, **17**, 201-214.
- MCDONNELL, A., 2001. Comparative Tertiary basin development in the Porcupine and Rockall Basins. Unpublished Ph.D Thesis, University College Dublin, 201 pp.
- MCKENZIE, D., 1978. Some remarks on the development of sedimentary basins. *Earth and Planetary Science Letters*, **40**, 25-32.
- MOORE, J.G. and SHANNON, P.M., 1995. The Cretaceous succession in the Porcupine Basin, offshore Ireland: facies distribution and hydrocarbon potential. In: SHANNON, P.M. (E.), *The Petroleum Geology of Ireland's Offshore Basins*. *Geol. Soc. Lond., Spec. Publ.*, **93**, 345-370.
- MORTENSEN, P.B., HOVLAND, M., BRATTEGARD, T. and FARESTVEIT, R., 1995. Deep water bioherms of the scleractinian coral *Lophelia pertusa* (L.) at 64 N on the

- Norwegian Shelf: structure and associated megafauna. *Sarsia*, **145**, 145-158.
- MULLINS, H.T., NEWTON, C.R., HEATH, K. and VANBUREN, H.M., 1981. Modern deep-water coral mounds north of Little Bahama bank: Criteria for recognition of deep-water coral bioherms in the rock record. *Journal of Sedimentary Petrology*, **51**, 999-1013.
- NADIN, P.A., KUSZNIR, N.J. and CHEADLE, M.J., 1997. Early Tertiary plume uplift of the North Sea and Faeroe-Shetland basins. *Earth and Planetary Science Letters*, **148**, 109-127.
- NEUMANN, A.C., KOFOED, J.W. and KELLER, G.H., 1977. Lithohierms in the Straits of Florida. *Geology (Boulder)*, **5**, 4-10.
- PEPPER, A.S. and CORVI, P.J., 1995. Simple kinetic models of petroleum formation. Part I: oil and gas generation from kerogen. *Marine and Petroleum Geology*, **12**, 291-319.
- POELCHAU, H.S., BAKER, D.R., HANTSCH, T., HORSFIELD, B. and WYGRALA, B.P., 1997. Basin simulation and the design of the Conceptual Model. In: WELTE, D.H., HORSFIELD, B. and BAKER, D.R. (Eds), *Petroleum and Basin Evolution*. Springer-Verlag, New York, 3-62.
- RITGER, S., CARSON, B. and SUESS, E., 1987. Methane-derived authigenic carbonates formed by subduction-induced pore-water expulsion along the Oregon/Washington margin; with Suppl. Data 87-02. *Geol. Soc. Am. Bull.*, **98**, 147-156.
- ROBERTS, H.H. and AHARON, P., 1994. Hydrocarbon-derived carbonate buildups of the northern Gulf of Mexico continental slope; a review of submersible investigations. In: AHARON, P. (Ed.), *Hydrocarbon seeps and vents. Geo-Marine Letters*, **14**, 135-148.
- SCHENK, H.J., HORSFIELD, B., KROOSS, B., SCHAEFER, R.G. and SCHWACHAU, K., 1997. Kinetics of petroleum formation and cracking. In: WELTE, D.H., HORSFIELD, B. and BAKER, D.R. (Eds), *Petroleum and Basin Evolution*, 233-269.
- SCOFFIN, T.P. and BOWES, G.E., 1988. The facies distribution of carbonate sediments on Porcupine Bank, Northeast Atlantic. *Sediment. Geol.*, **60**, 125-134.
- SCOTCHMAN, I.C., 2001. Petroleum geochemistry of the Lower and Middle Jurassic in Atlantic margin basins of Ireland and the UK. In: P.M. Shannon, P. Haughton, D.V. Corcoran, (Eds), *The Petroleum Exploration of Ireland's Offshore Basins*, Geological Society, London, Special Publication **188**, 31-60.
- SHANNON, P.M. and JACOB, A.W.B. 1988. Crustal structure onshore to offshore Ireland: Development from Palaeozoic to Recent time. *Annales Geophysicae*, **16**, C109.
- SHANNON, P.M. and NAYLOR, D., 1998. An assessment of Irish offshore basins and petroleum plays. *Journal of Petroleum Geology*, **21**, 125-152.
- SOAVE, G., 1972. Equilibrium constants from a modified Redlich-Kwong equation of state. *Chem. Eng. Sci.*, **27**, 1197-1203.
- STETSON, T.R., HERSEY, J.B. and KNOTT, S.T., 1963. Shallow structures of the Blake Plateau. *Transactions - American Geophysical Union*, **44**, 64.
- STROMGREN, T., 1974. The use of a weighted arithmetic mean for describing the sediments of a landlocked basin (Borgenfjorden, Western Norway). *Deep-Sea Research and Oceanographic Abstracts*, **21**, 155-160.
- SUESS, E. and WHITICAR, M.J., 1989. Methane-derived CO<sub>2</sub> in pore fluids expelled from the Oregon subduction zone. *Palaeogeography, Palaeoclimatology, Palaeoecology*, **71**, 119-136.
- SWEENEY, J.J. and BURNHAM, A.K., 1990. Evaluation of a simple model of vitrinite reflectance based on chemical kinetics. *AAPG Bull.*, **74**, 1559-1570.
- SYLTA, O., 1991. Modelling of secondary migration and entrapment. In: ENGLAND, W.A. and FLEET, A.J. (Eds), *Petroleum migration. Geol. Soc. Lond., Spec. Pub.*, **59**, 111-122.
- TATE, M.P., 1993. Structural framework and tectono-stratigraphic evolution of the Porcupine Seabight Basin, offshore western Ireland. *Marine and Petroleum Geology*, **10**, 95-123.
- TATE, M.P. and DOBSON, M.R., 1988. Syn- and post-rift igneous activity in the Porcupine Seabight Basin and adjacent continental margin of W of Ireland. In: PARSON, L.M. (Ed.), *Early Tertiary Volcanism and the Opening of the NE Atlantic*, *Geol. Soc. Lond., Spec. Pub.*, **39**, 309-334.
- TEGELAAR, E.W. and NOBLE, R.A., 1993. Kinetics of hydrocarbon generation as a function of the molecular structure of kerogen as revealed by pyrolysis-gas chromatography. *Organic Geochemistry*, **22**, 543-574.
- VIANA, M.S.S., MABESOONE, J.M. and NEUMANN, V.H., 1994. Lacustrine phases in the Araripe Basin (NE Brazil). 14th international sedimentological congress; abstracts. International Association of Sedimentologists Comparative Sedimentology Division, S6.11-S6.12.
- WILSON, J.B., 1979. 'Patch' development of the deep-water coral *Lophelia pertusa* (L.) on Rockall Bank. *J. Mar. Biol. Ass. UK*, **59**, 165-177.